

R22: A Multi-Functional Imager for TOF and High Performance Video Applications Using a Global Shuttered 5µm Cmos Pixel.

Peter Centen¹, Juul v.d Heijkant¹, Jeroen Rotte¹, Klaas Jan Damstra¹,
Assaf Lahav², Adi Birman², Steffen Lehr³, Sabine Roth³, Ruud van Ree¹

1) Grass Valley, Breda, the Netherlands, 2) TowerJazz, Haifa, Israel, 3) Viimagic, Villingen, Germany
peter.centen@grassvalley.com; Grass Valley, kapittelweg 10, 4827HG Breda, The Netherlands;
Cell: +31613679702; Fax+ 31 76 5721548;

Abstract

In this paper we present an imager designed for high performance video applications and Time of Flight [1]. The voltages and pulses applied to the global shutter gate (GS) and the transfer gate (TG) determine whether the pixel operates as a video-pixel or a TOF-pixel.

Using a pinned photodiode for Time of flight is not straight forward. Essential is a long duration for the TG and GS with respect to the duration of the LED pulse. In the experiments IR LED light pulses are used.

The pixel and the driving pulses

Figure 1. Detailed schematic of the 5T global shuttered pixel. GS is the global shutter gate. The VSS_GS is the global shutter drain and the transfer gate is depicted as TG. C_{fd} represents the floating diffusion, FD. The pinned-photodiode (PD) is the light collecting element. In contrast with [2] the PD is not heavily shaped for driving field nor has the pixel an adapted architecture [2,3,4,5,6]. As such the pixel is just an ordinary “video” pixel with the FD as intermediate storage node.

Figure 2. Oscilloscope photo of the driving pulses for the global shutter gate (GS) and the transfer gate (TG). The pulses that drive the LED IR-light source are shown inverted. GS and TG are each other's inverse. With this driving pattern TOF operation is achieved.

Pixel output versus LED light pulse position in TG-window

Figure 3: The LED-pulse is projected to an object and reflected back to the imager. To explore the TOF capabilities of the pixel, in an easy fashion, the pixel output are measured as a function of the position of the LED-pulse in the TG-window. The time delay between TG and LED-pulse (dT) is converted in an equivalent distance ($dD=C*dT/2$). The transfer gate (TG) is high during 1µs and low during 1µs (Figure 2, 3), giving a periodicity of 2µs. The global shutter (GS) is high when the transfer gate is low and vice versa. The duration of TG is long enough to enable sufficient charge transfer from PD across TG to the FD. The LED is on during 240ns of the 2µs period.

Figure 4: between 0m and 50m (**A**) the offset+background is measured. From 50m to 90m (**B**) the output signal is linear proportional with the time difference and hence with distance. The signal between 100m and 200m (**C**) is the summation of the offset+background + total-reflected light. The right descending slope of the graph is slightly parabolic and less usable for TOF images.

A TOF distance map can be generated by positioning the TG/GS pulses, with respect to the LED IR-illuminator pulses. In the end 3 measurements are needed for calculating the distance: $D=D_{max} * (B-A)/(C-A)+D_0$. (Figure 4, A,B,C). D_{max} is determined by the pulse-width of the LED-light. The position of a reference surface is D_0 .

Next the responses of 6 consecutive pixels are measured in row 124 as a function of the position of the IR LED-pulse in the TG window. In **Figure 5** the 6 individual pixel outputs are plotted and in **Figure 6** the pixel amplitudes are normalized by using respective $(B - A)/(C - A)$. The linearity is good when the LED pulse is crossing the rising edge of TG and a large variance when the LED pulse is crossing the falling edge of TG.

The depth map

The basis of the depth map is the time difference between the moment of sending out the LED light pulse and the time-instant the LED pulse is returned and projected on the imager. The time difference is the sum of Time (Of Flight) and the (variable) delay in the on chip driving electronics, like the propagation delay of the TG and GS pulses. A depth/timing calibration is needed. A positive side-effect of the depth calibration is a rather accurate measurement of the electrical properties of the driving electrons and pulse distribution on chip. A parabolic correction in both Horizontal- and Vertical-direction works fine. The correction range needed for this imager, is along the vertical axis about 19ns and for the horizontal axis 4ns. A calibration on a pixel by pixel basis is even better. The depth maps in the Fig 7 and 8 are already calibrated depth maps.

Figure 7: The left part is a normal image of 4 objects with a curtain in the background. The middle part is a depth map of the 4 objects which are positioned at different distances. And the right part of figure 7 is the mapping between color and depth in [cm].

Figure 8: is a depth map of Ernie, a doll.

Table 1: Some references to dedicated TOF pixels and their pixel dimensions and this imager.

Table 2: Some device and performance parameters. They show that the sensitivity and noise levels are indeed at “video” performance.

Conclusions

In this paper we have shown the possibility of TOF with a 5-transistor global shutter pixel that reaches a good performance as well in visible imaging. To expand it towards a fully fledged TOF imager one can apply an odd/even row addressing (modulo 2) for separately positioning the TG/GS timing with respect to the LED timing. With 2 consecutive images one obtains the background, total reflected and depth for TOF calculation. With modulo 3 addressing of the rows the background, total reflected and depth is obtained in one image.

References

- [1] Oggier, *Image Sensor technologies for 3D time of flight range imaging*, **International Image Sensor Workshop**, Norway, 2009.
- [2] Tubert et.al, *High Speed Dual Port Pinned-Photodiode for Time Of Flight Imaging*, **International Image Sensor Workshop**, Norway, 2009.
- [3] Van Nieuwenhove et. al, *Photonic Demodulator With Sensitivity Control*, **IEEE Sensors Journal**, 2007, pp 317–318.
- [4] Kawahito et.al, *A CMOS Time-of-Flight Range Image Sensor With Gates-on-Field-Oxide Structure*, **IEEE Sensors Journal**, 2007, pp 1578 – 1586.
- [5] Yoshimura et.al., *A 48 kframe/s CMOS image sensor for real-time 3-D sensing and motion detection*. **ISSCC 2001**, pp: 94 - 95, 436.
- [6] Buttgen et.al., *Demodulation Pixel Based on Static Drift Fields*, **IEEE Transactions on Electron Devices**, 2006 , pp 2741 – 2747.

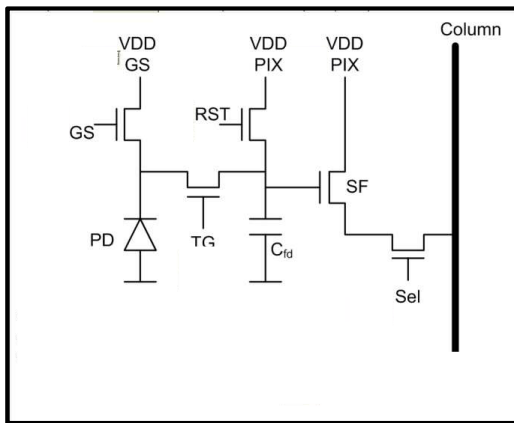


Figure 1: schematic of the 5T pixel

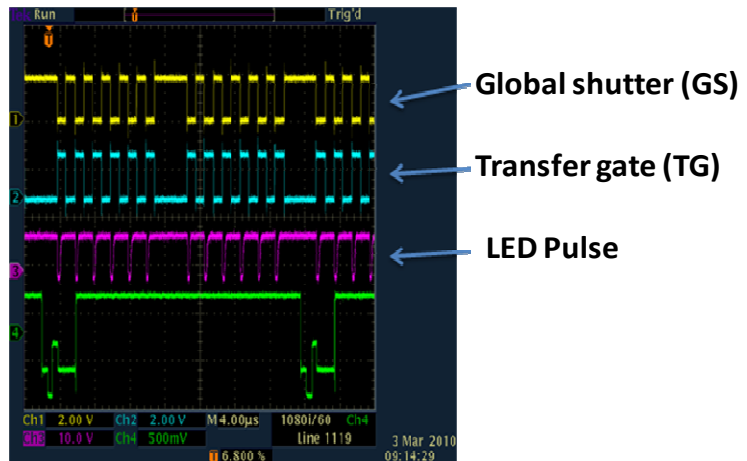


Figure 2: Driving voltages for global shutter gate (GS), Transfer Gate (TG) and LED IR-light driving pulses

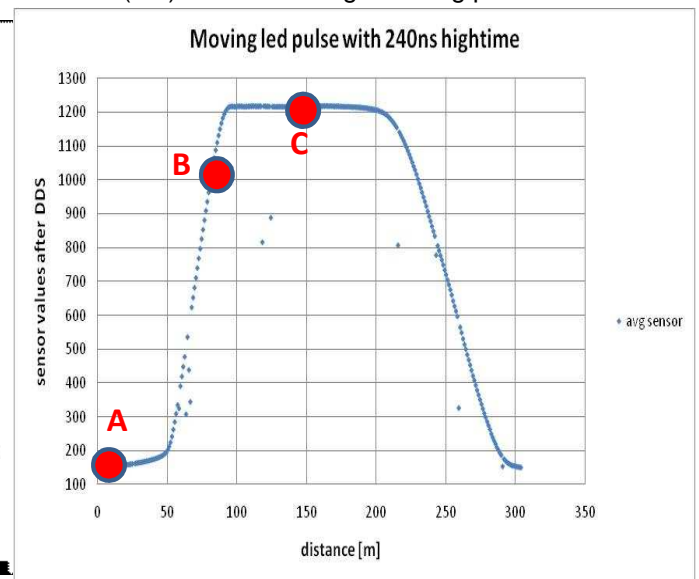
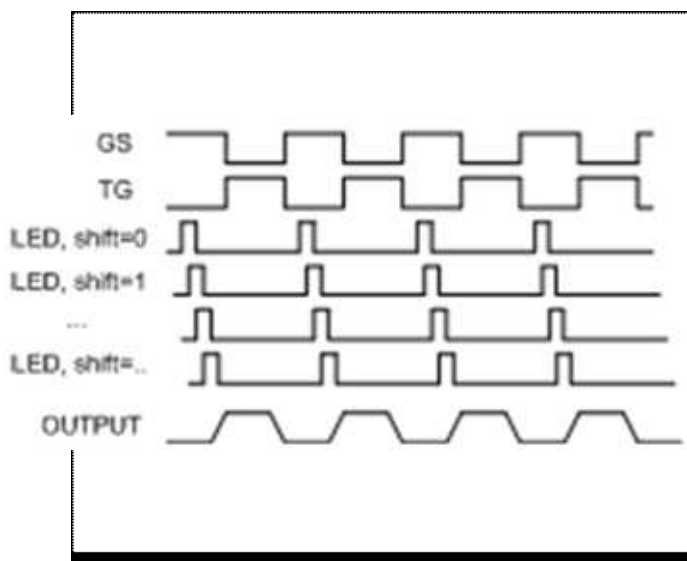


Figure 3: On the **left** is a timing diagram for the shift of the LED-pulse through the TG-window to measure the response of the pixel. **Figure 4:** An example of the pixel response is plotted in the **right** graph.

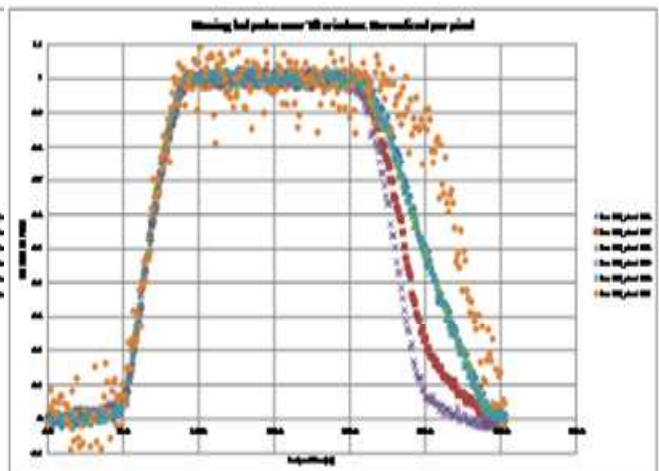
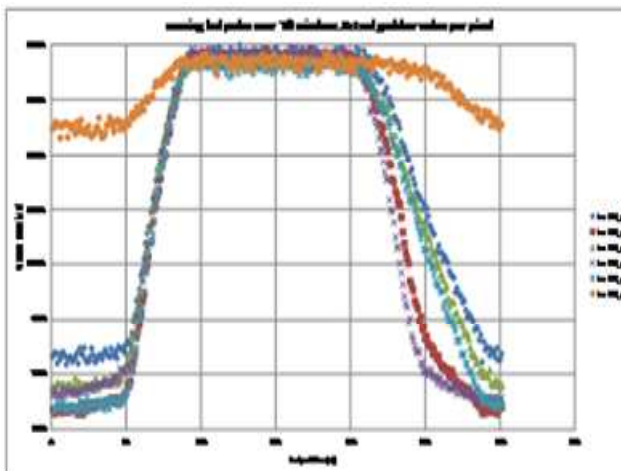


Figure 5: The pixel output of 6 consecutive pixels on row 124 as a function of the position of the LED-pulse in the TG window. **Figure 6:** The raw pixel output is plotted in the **left** graph. The normalized (0...1) pixel output is plotted in the **right** graph.

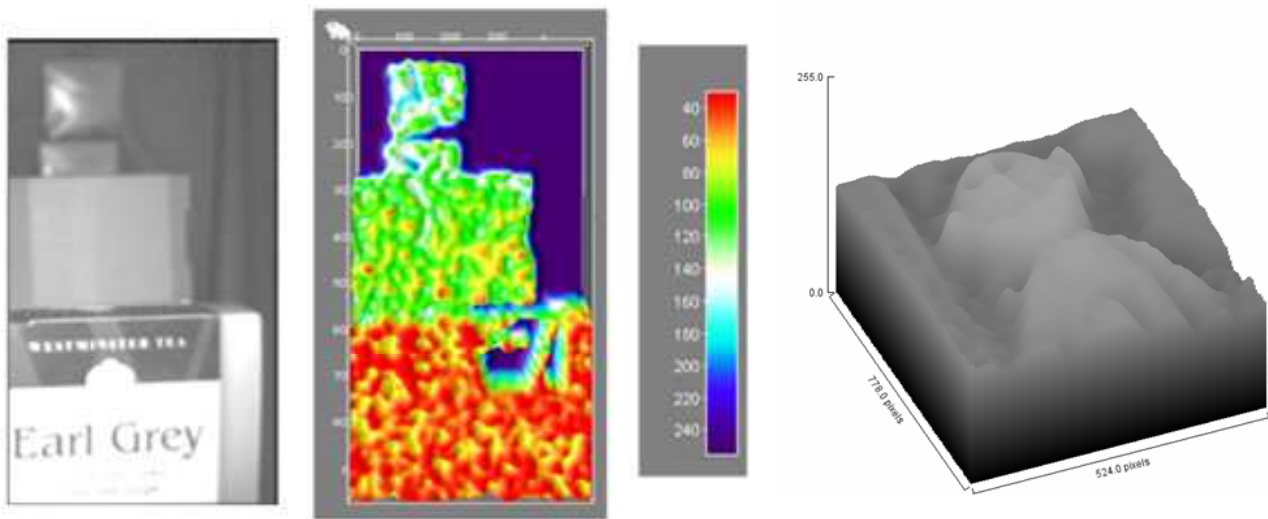


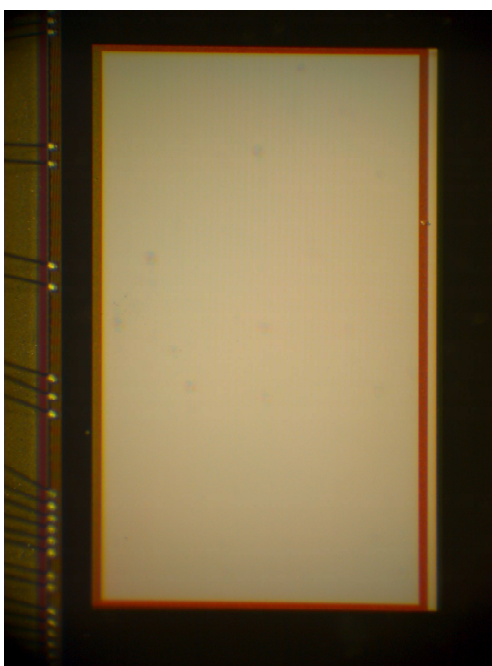
Figure 7: a depth map of some objects. Left a normal image, in the middle a depth map of some objects, on the right the relation between [cm] distance and color.

Figure 8: Ernie a doll

Literature	Pixel size [$\mu\text{m} \times \mu\text{m}$]		Technology	0.18 μm 4m1p
Buttgen, SPIE, 2004	50x50		Chip Size	5mm (H) x 10mm (V)
Yoshimura, ISSCC 2001	46.4x54		Pixels	574 (H) x 960 (V)
Nieuwenhove, IEEE Sensors, 2007	30x30		Pixel size	5x5 μm
Kawahito, IEEE Sensors, 2007	15x15		Clock frequency	74MHz
Tubert, IISW2009	11.2x11.2		Read Noise	6e
This paper	5x5		Sensitivity in Green	55 kel/luxsec
			Qmax	15kel

Table 1: TOF pixel sizes

Table 2: Performance and device summary



Chip Photograph